Available online at www.jourcc.com

Journal homepage: www.JOURCC.com

Journal of Composites and Compounds

$AlFeO_3@SiO_2@SO_3H$ as a magnetic nanocatalyst for the synthesis of mono/bis-dihydropyrimidin-2-ones and dihydropyridines as pharmaceutically active compounds

Mohammad Ali Bodaghifard [ab], Najmieh Ahadi [b], Faranak Ebrahimi [a], Mahdia Hamidinasab [a]**

[a] *Department of Chemistry, Faculty of Science, Arak University, 38156-88138, Arak, Iran*
[b] *Institute of Nanosciences and Nanotechnology, Arak University, 38156-88138, Arak, Iran*

ABSTRACT

In this research, the preparation of a reusable $AlFeO_3@SiO_2@SO_3H$ nanostructure as a perovskite-based magnetic nanomaterial is described. The structure of prepared AlFeO3@$SiO_2@SO_3H$ was characterized by FT-IR, XRD, FE-SEM, EDS, TGA, and VSM analyses. The prepared acidic hybrid nanocatalyst showed high thermal stability and used as an efficient magnetic nanocatalyst in the synthesis of 3,4-dihydropyrimidin-2-one, and mono/bis 1,4-dihydropyridine derivatives as pharmaceutically active heterocycles under solvent free conditions. High efficiency of procedure, good yields, short reaction times, magnetic recovery and reusability of nanocatalyst, high thermal stability of catalyst, and environmentally benign conditions are highlights of this new protocol.

Peer review under responsibility of UGPH.

ARTICLE INFORMATION

Article history:
Received 18 December 2022
Received in revised form 20 February 2023
Accepted 25 March 2023

Keywords:
Magnetic nanocatalyst
Perovskite structure
Biginelli reaction
Hantzsch reaction
Pharmaceutical compounds
Green synthesis

1. Introduction

The main challenge of modern medicinal chemistry is synthesis of novel bioactive molecules that can be potentially used as drugs [1]. Molecules containing 3,4-dihydropyrimidin-2-one (DHPMs) and 1,4-dihydropyridine (DHP) structures are very important in pharmaceutical and medicinal chemistry due to their diverse properties (Figure 1), such as anticancer [2-5], antibacterial [6, 7] and many other pharmacological activities [8, 9]. 1,4-DHP have primarily been used as calcium channel modulators [10] and 1,2,3,4-tetrahydropyrimidines have also been evaluated as calcium channel modulating agents due to their structural similarity to 1,4-dihydropyridines [11]. MCRs engage three or more components simultaneously, resulting in products that incorporate the elements of all starting materials in their final structures. This integrative nature of MCRs is attractive when a rapid increase in molecular diversity is desired. Using a combinatorial approach, sets of components can be systematically distributed in arrays of reactions to generate interactions on a common MCR-product scaffold. MCRs have many advantages as they save precious time, simplifies the synthesis and diminishes the work-up procedures [12, 13]. Hantzsch in 1882 and Biginelli in 1893, reported one-pot multicomponent reactions for the synthesis of 1,4-dihydropyridine and dihydropyrimidinone structures, respectively [14]. Hantzsch condensation led to the formation of dihydropyridines *via* the reaction of aldehyde, two equivalents of a β-ketoester, and source of nitrogen such as ammonium acetate or ammonia and Biginelli condensation reaction between an aldehyde, urea/thiourea and a carbonyl compound is the most popular strategy for the synthesis of dihydropyrimidinones. Acetoacetate esters and aromatic aldehydes were the two components common in both reactions. The development of new, sustainable chemical processes for the synthesis of these biologically active molecules accelerated via multicomponent reactions using heterogeneous catalysis strategy such as efficient magnetic nanocatalyst [15-20].

There are many reports for the synthesis of DHPs and DHMPs in the presence of NPs as catalysts. For examples, Ch-Rhomboclase nanoparticles [18], $CoFe_2O_4$ @ SiO_2-NH_2-Co (II) [21], MIL-101-SO_3H [22], CuO [23], COF-IM-SO_3H [24] are used as catalysts for the synthesis of DHPs and DHMPs.

There has been research interest in perovskite type oxide materials (ABO_3) such as $TbMnO_3$, $BiFeO_3$, $NiTiO_3$, $BaMnO_3$, and $AlFeO_3$ [25-27]. These materials exhibit multiferroic property (magnetoelectric, ferroelectric properties), high chemical stability, good sensitivity to the visible light, and have gained significant technological attention specially in photoelectric conversion and photochemical degradation [28, 29]. Ferrite-based perovskites, such as $AlFeO_3$, have vast potential due to their magnetic behaviour leading to enhanced recovery from reactions. Both aluminium and iron are earth-abundant elements and non-carcinogenic which makes $AlFeO_3$ an eco-friendly and cost-effective material

* *Corresponding author: Mohammad Ali Bodaghifard; E-mail: mbodaghi2007@yahoo.com, Mahdia Hamidinasab; E-mail: mahdiahamidinasab@yahoo.com*
DOR:
https://doi.org/10.61186/jcc.5.1.2

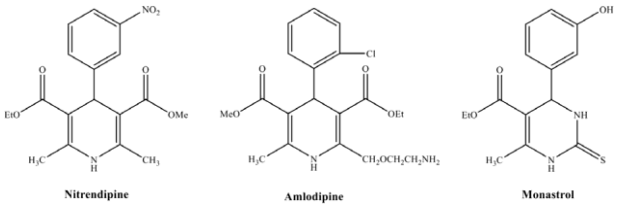

Fig. 1. Examples of some pharmacologically active dihydropyridine and dihydropyrimidinone structures.

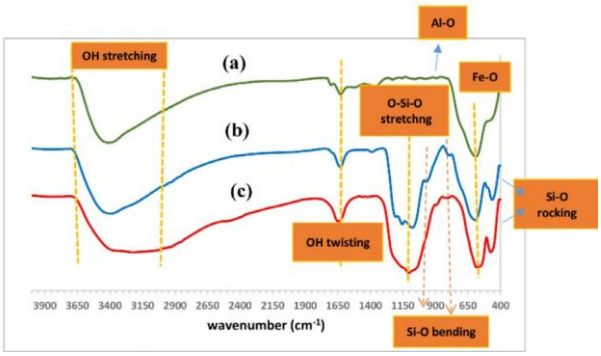

Fig. 2. The FT-IR spectra of (a) $AlFeO_3$, (b) $AlFeO_3@SiO_2$, and (c) $AlFeO_3@SiO_2@SO_3H$ MNPs.

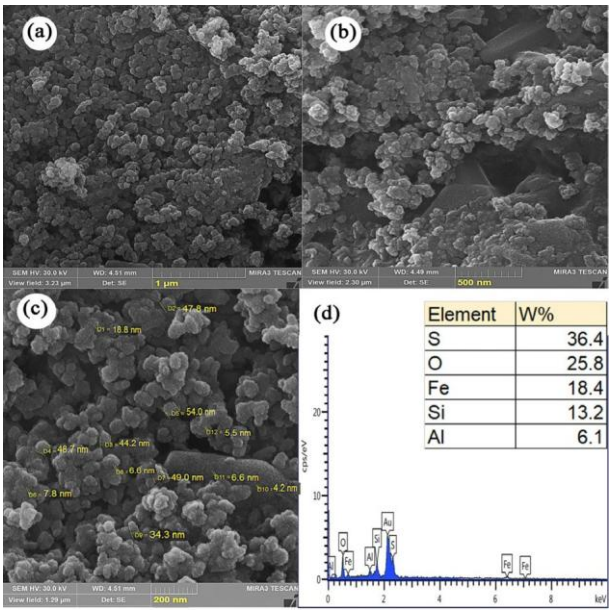

Fig. 4. (a, b, c) The FE-SEM (200, 500 nm and 1 µm), and (d) EDX analysis of $AlFeO_3@SiO_2@SO_3H$ MNPs.

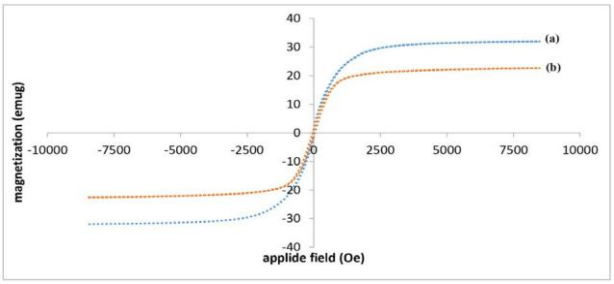

Fig. 6. VSM analysis of $AlFeO_3@SiO_2@SO_3H$ MNPs.

[26]. However, there are few studies on the catalytic activity of $AlFeO_3$ powders. $AlFeO_3$ has orthorhombic or rhombohedral structure and is expected to show good catalytic or photocatalytic performance along with its magnetic recoverability [30].

In continuation of our efforts for development of green procedures to design and synthesis of DHPs and DHMPs [31, 32], herein, we have

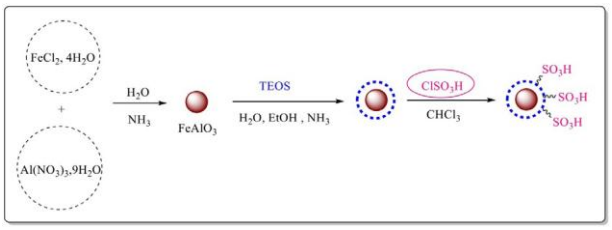

Scheme. 1. The synthetic pathway for $AlFeO_3@SiO_2@SO_3H$ MNPs.

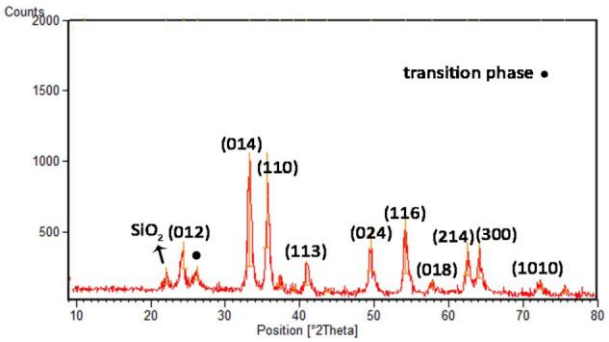

Fig. 3. The XRD patterns of $AlFeO_3@SiO_2@SO_3H$ nanostructure.

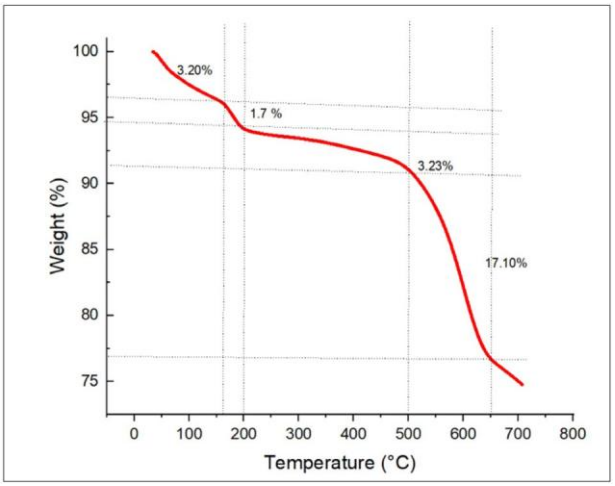

Fig. 5. TGA analysis of $AlFeO_3@SiO_2@SO_3H$ MNPs.

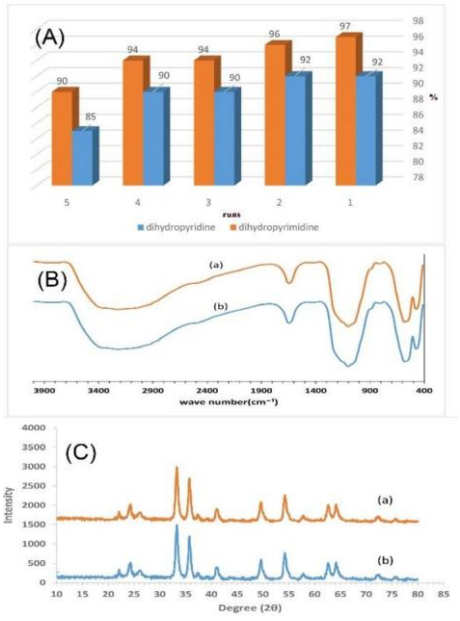

Fig. 7. Reusability of $AlFeO_3@SiO_2@SO_3H$ for 5 times (A), FT-IR spectra of fresh (a) and reused (b) catalyst (B), and the XRD patterns of fresh (a) and reused (b) catalyst after 5 runs.

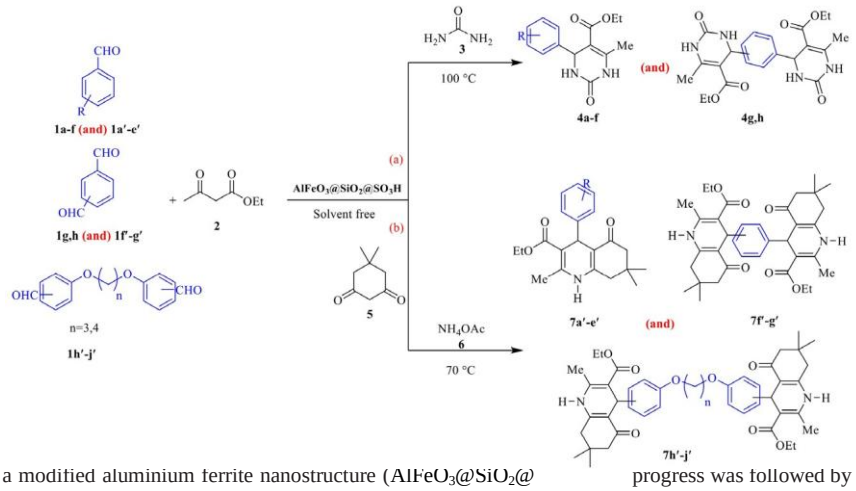

Scheme. 2. Synthesis of (a) mono/bis-3,4-dihydropyrimidin-2-ones, and (b) mono/bis-1,4-dihydropyridines in the presence of AlFeO3@SiO_2@SO_3H MNPs.

prepared a modified aluminium ferrite nanostructure ($AlFeO_3$@SiO_2@SO_3H) as a perovskite-based magnetic nanomaterial and considered its catalytic activity in Hantzsch and Biginelli multicomponent reactions (Scheme 2).

2. Material and methods

All chemicals were purchased from Merck and Fluka chemical companies. Dialdehydes (**1h'-j'**) were synthesized in the laboratory according to the reported synthetic method [33]. The Fourier-transform infrared (FT-IR) spectra were recorded by the Bruker alpha device in range 400-4000 cm^{-1}. Thermogravimetric analysis (TGA) of $AlFeO_3$@SiO_2@SO_3H MNPs was performed by the device (TA, Q600 model, Germany) under Ar atmosphere with rate 10 °C/min. The morphology and shape of $AlFeO_3$@SiO_2@SO_3H MNPs was elucidated by field emission electron microscopy (FE-SEM) using TESCAN MIRA model. The presence of elements in structure of $AlFeO_3$@SiO_2@SO_3H MNPs was performed by X-ray energy diffraction spectrometer (EDX). The crystalline structure of $AlFeO_3$@SiO_2@SO_3H MNPs was investigated by X-ray diffraction spectroscopy (XRD) using Philips PW1730 powder diffraction (XRD) diffractometer (Cu-Kα radiation and λ= 0.15406) in the range of Bragg angle (2θ= 10-80) using 0.05° as the step length. The magnetic property of prepared nanostructure was studied by vibrating sample magnetometer (VSM, model: 730 VSM system) at room temperature. The reaction progress was followed by thin layer chromatography (TLC) using silica gel coated aluminum plates and using n-hexane/ethylacetate eluents. Melting points of the synthesized heterocyclic compounds were measured using an electrothermal 9100 digital apparatus. The ^{1}H-NMR and ^{13}C-NMR spectra were recorded by Bruker Avence (300 and 75 MHz respectively) in DMSO-d_6 solvent. The mass spectra of new products were recorded by agilent 5975C model.

Table 1.
The optimization of reaction conditions for the synthesis of 3,4-dihydropyrimidin-2-one (**4a**)

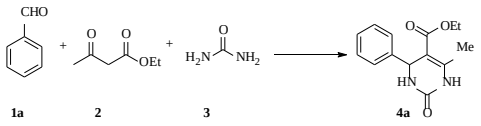

Entry	Catalyst (mg)	Solvent	Temperature (°C)	Time (min.)	Yield[a] (%)
1	10	EtOH	Reflux	75	78
2	10	H_2O	Reflux	85	70
3	10	EtOH:H_2O (1:1)	Reflux	78	85
4	10	Solvent free	100	45	97
5	5	Solvent free	100	68	85
6	8	Solvent free	100	60	86
7	20	Solvent free	100	45	96
8	10	Solvent free	70	87	75
9	10	Solvent free	R.T	130	65
10	-	Solvent free	100	360	17

[a] Isolated yield. benzaldehyde (1mmol, 0.14 g), urea (1.5 mmol, 0.09 g), Ethyl acetoacetate (1mmol, 0.13 mL), and the $AlFeO_3$@SiO_2@SO_3H nanocatalyst.

2.1. Preparation of $AlFeO_3$@SiO_2@SO_3H nanostructure

The modified $AlFeO_3$ MNPs was prepared in three steps as follows.

2.1.1. Preparation of $AlFeO_3$ MNPs

The co-precipitation method was used for the preparation of $AlFeO_3$ [34]. The $Al(NO_3)_3.9H_2O$ (5 mmol, 1.87 gr) and $FeCl_2.4H_2O$ (5 mmol, 0.99 g) were dissolved in the deionized water (50 mL) and stirred for 2 h at 95 °C under N_2 atmosphere. Then, NH^4OH (10%) was added to solution to adjust pH=10 and stirred again for 2 h. The brown black sediment was separated by an external magnet, washed by deionized water (100 mL), EtOH (10 mL), and finally dried in a vacuum oven at 70 °C.

2.1.2 Preparation of silica-coated $AlFeO_3$ MNPs ($AlFeO_3$@SiO_2)

The surface of $AlFeO_3$ NPs was coated by TEOS *via* Stöber method [31]. 1 g of $AlFeO_3$, EtOH (20 mL), H_2O (1.5 mL), and NH_4OH (0.4 mL) were poured in a round bottom flask (50 mL) and were sonicated for 30 min. Then 1.4 mL of TEOS was added to the mixture and stirred at room temperature for 24 h under N_2 atmosphere. The magnetic precipitation was isolated by an external magnet, washed by deionized water (100 mL), and dried in a vacuum oven at 70 °C.

2.1.3. Preparation of sulfonic acid-decorated $AlFeO_3$@SiO_2 MNPs

Table 2.
Synthesis of 3,4-dihydropyrimidin-2-ones in the presence of AlFeO3@SiO_2@SO3H nanocatalyst.

Entry	Aldehydes	Product	Time (min.)	Yield[a] (%)	M.p [Ref]
1	C_6H_5CHO	**4a**	40	97	218-216 [39]
2	2-OCH_3-C_6H_4CHO	**4b**	80	90	258-260 [39]
3	4-OCH_3-C_6H_4CHO	**4c**	50	93	206-209 [40]
4	2,4-$Cl_2C_6H_3CHO$	**4d**	75	95	236-238 [32]
5	4-Cl-C_6H_4CHO	**4e**	35	93	202-204 [39]
6	4-CN-C_6H_4CHO	**4f**	15	89	230-232 [41]
7	terphetaldehyde	**4g**	90	87	274 [42]
8	Isoterphetaldehyde	**4h**	90	83	293-295 [42]

[a] Isolated yield. Arylaldehyde (1mmol), ethyl acetoacetate (1mmol, 0.13 mL), urea (1.5 mmol, 0.09 g), and $AlFeO_3$@SiO_2@SO_3H nanocatalyst (10 mg) under solvent free condition at 10 °C.

(AlFeO$_3$@SiO$_2$@SO$_3$H)

AlFeO$_3$@SiO$_2$@SO$_3$H nanostructure was fabricated by using a reported procedure [35]. AlFeO$_3$@SiO$_2$ (1 g) was dispersed in dry CH_3Cl (20 mL) for 20 min. A solution of chlorosulfonic acid (0.3 mL) in dry CH_3Cl (10 mL) was slowly added to AlFeO$_3$@SiO$_2$ suspension during a period of 30 minutes and stirred for 2 h. Then, AlFeO$_3$@SiO$_2$@SO$_3$H was separated by an external magnet, washed by dry CH_3Cl (10 mL), EtOH (10 mL), and dried in a vacuum oven at 70 ℃.

2.2. Acid-base titration of AlFeO$_3$@SiO$_2$@SO$_3$H

The acidity of AlFeO$_3$@SiO$_2$@SO$_3$H estimated by the back titration method. The mixture 2 mL of NaOH (0.01 M) and 0.02 g of AlFeO$_3$@SiO$_2$@SO$_3$H were stirred for 30 min. The magnetic nanoparticles were separated by an external magnet. In continue, back-titration by HCl (0.01 M) was carried out for the solution in the presence of phenolphthalein indicator for three times. The average value for the concentration of dissociable sulfonic acid groups was calculated. The acid-base titration results revealed that 0.31 mmol/g acidic groups were immobilized on the surface of AlFeO$_3$@SiO$_2$@SO$_3$H MNPs.

2.3. General procedure for the synthesis of 3,4-dihydropyrimidin-2-ones (4a-h)

Aryl aldehyde (1 mmol), ethylacetoacetate (1 mmol), urea (1.5 mmol), and 0.01 g of AlFeO$_3$@SiO$_2$@SO$_3$H MNPs was poured in a test tube and heated under solvent free condition at 100 °C. The progress of reaction was followed by TLC using n-hexane/ethylacetate (2:1) as an eluent. At the end of the reaction, the mixture was diluted by 20 mL EtOH and nanocatalyst was separated by an external magnet. The solution was cooled to form pure crystalline products.

2.4. General procedure for the synthesis of 1,4-dihydropyridines (7a-j)

A mixture of aryl aldehyde (1 mmol), ethyl acetoacetae (1 mmol), dimedone (1 mmol), and ammonium acetate (1.5 mmol) were heated in the presence of 0.01 g of AlFeO$_3$@SiO$_2$@SO$_3$H under solvent free condition at 100 °C. The progress of reaction was followed by TLC using n-hexane/ethylacetate (2:1) as an eluent. After completion of the reaction, the mixture was diluted by 20 mL EtOH and nanocatalyst was isolated by an external magnet. Then, solution was cooled to room temperature to form pure crystalline 1,4-dihydropyridine derivatives.

Table 3.
The optimization of reaction condition for the synthesis of 1,4-dihydropyridine (7a').

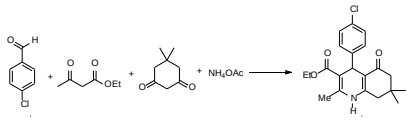

Entry	Catalyst (mg)	solvent	Temperature (°C)	Time (min.)	Yield[a] (%)
1	5	Solvent free	100	60	80
2	5	EtOH	Reflux	78	78
3	5	H_2O	Reflux	90	68
4	5	EtOH:H_2O(1:1)	Reflux	83	71
5	8	Solvent free	100	56	80
6	10	Solvent free	100	30	95
7	20	Solvent free	100	29	93
8	10	Solvent free	70	65	85
9	10	Solvent free	R.T	200	63
10	-	Solvent free	100	360	21

[a] Isolated yield. Ethyl acetoacetate (1mmol, 0.13 mL), benzaldehyde (1mmol, 0.14 g), Dimedone (1 mmol, 0.14 g), ammonium acetate (1.5 mmol, 0.09 g), and the AlFeO$_3$@SiO$_2$@SO$_3$H nanocatalyst.

3. Result and discussion

The synthetic pathway of AlFeO$_3$@SiO$_2$@SO$_3$H nanostructure is presented in scheme 1. AlFeO$_3$ MNPs was prepared by the co-precipitation method and coated by TEOS to achieve the AlFeO$_3$@SiO$_2$ MNPs. By reaction with chlorosulfonic acid, the surface of AlFeO$_3$@SiO$_2$ was decorated by sulfonic acid groups. Then, the prepared AlFeO$_3$@SiO$_2$@SO$_3$H nanostructure was characterized by the FT-IR, XRD, FE-SEM, EDS, TGA and VSM analyses.

3.1. Characterization of AlFeO$_3$@SiO$_2$@SO$_3$H MNPs

The FT-IR spectra of AlFeO$_3$ (a), AlFeO$_3$@SiO$_2$ (b), and AlFeO$_3$@SiO$_2$@SO$_3$H MNPs shown in Figure 2. The absorption bands in ranges 300-3500 cm^{-1} and 1628 cm^{-1} are attributed to -OH stretching and twisting vibrations of physically adsorbed water and solvents in structures. In addition, the weak band at 700-900 cm^{-1} is belonged to Al-O (Fig.1a) [36]. The absorption bands of Si-O stretching, bending, and rocking are appeared at 1100 (O-Si-O stretching vibration), 970 and 850 (Si-O bending vibrations), and 475 (Si-O rocking) cm^{-1} (Fig. 1a, b). In addition, the vibration of SO_3H is overlapped with O-Si-O stretching vibration at 1000-1200 cm^{-1} [35]. The obtained results prove the presence of functional groups and successful construction of desired AlFeO$_3$@SiO$_2$@SO$_3$H nanostructure.

The XRD patterns of AlFeO$_3$@SiO$_2$@SO$_3$H shows 12 peaks in 2θ= 22.03°, 24.27°, 27.05°, 33.31°, 35.70°, 41.03°, 49.57°, 54.18°, 58.20°, 62.62°, 64.17°, and 72.26° (Figure 3). The peaks in 2θ=24.27°, 33.31°, 35.70°, 41.03°, 49.57°, 54.18°, 58.20°, 62.62°, 64.17°, and 72.26° attributed to Miller planes (012), (104), (110), (113), (024), (116), (018), (214), (320), and (1010), respectively and confirm its structure [37]. The peak observed at 2θ=27.05° can be related to the transition phase (the rhombohedral to the orthorhombic structure) as reported in the literature [38]. The appearance of peak at 2θ= 22.03° is according to amorphous SiO_2 and confirms the formation of SiO_2 shell on AlFeO$_3$ nanoparticles.

The field emission scanning electron microscopy (FE-SEM) was used to elucidate the morphology and size of AlFeO$_3$@SiO$_2$@SO$_3$H MNPs (Figure 4a, b and c). Resulting images confirm that nanoparticles have spherical shape with some agglomerates. The size distributed from 8 to 48 nm. The EDS analysis confirms the presence of iron (Fe), aluminium (Al), oxygen (O), and sulfur (S) in AlFeO$_3$@SiO$_2$@SO$_3$H structure (Figure 4d). The results prove the successful immobilization of –SO$_3$H groups on AlFeO$_3$@SiO$_2$ nanostructure.

The thermal stability of AlFeO$_3$@SiO$_2$@SO$_3$H MNPs was investigated by the TGA analysis (Figure 5). The TGA analysis show four steps of weight loss in the range of 25 to 700 °C. The 5% loss weight at T<200 °C can be attributed to the removal of physically adsorbed water and organic solvents. In addition, loss weight of 20% in the range 200 to 650 °C is belongs to the removal of SO_3H groups loaded on AlFeO$_3$@SiO$_2$ NPs. The amount of SO_3H loaded on AlFeO$_3$@SiO$_2$ NPs was estimated about 0.28 mmol/g which is in accordance to the back titration result.

The magnetic property of AlFeO$_3$ (a) and AlFeO$_3$@SiO$_2$@SO$_3$H nanostructure was studied by the vibrating sample magnetometry (VSM) analysis in the range of ±8000 Oe at room temperature (Figure 6). The hyestresis loop (like S) shows the magnetic saturation (Ms) about 30 Oe for (AlFeO$_3$) and 18 Oe for AlFeO$_3$@SiO$_2$@SO$_3$H. The decrease of magnetic property of AlFeO$_3$@SiO$_2$@SO$_3$H confirm that AlFeO$_3$ has successfully coated with silica layer and modified with sulfonic acid groups.

3.2. Investigation on catalytic activity of AlFeO$_3$@SiO$_2$@SO$_3$H

The catalytic activity of $AlFeO_3@SiO_2@SO_3H$ nanostructure was investigated in the synthesis of mono/bis-3,4-dihydropyrimidin-2-one (**4a-h**) and mono/bis-1,4-dihydropyridine (**7a'-j'**) derivatives (Scheme 2).

3.2.1. Catalytic activity of $AlFeO_3@SiO_2@SO_3H$ in the synthesis of 3,4-dihydropyrimidin-2-one derivatives (4a-h)

A model reaction of benzaldehyde (1mmol, 0.14 g), ethyl acetoacetate (1mmol, 0.13 mL), and urea (1.5 mmol, 0.09 g) was selected to optimize the reaction condition (Table 1). Three eco-friendly solvents including H_2O, EtOH:H_2O (1:1), EtOH, and solvent free condition were studied. The best result was achieved in solvent free condition (Table 1, Entries 1-4). Then, 5, 8, 10, and 20 mg of catalyst were examined under solvent free condition at 100 °C (Table 1, Entries 4-7) and results showed that the increasing of catalyst from 5 to 10 mg have positive effect on time and yield of reaction. However, the further increasing of catalyst from 10 to 20 mg have not positive effective on time and yield of reaction. So, the optimal amount of catalyst was found to be 10 mg (Table 1, Entries 4). Finally, the effect of different temperatures such as room temperature, 70, and 100 °C was studied on model reaction (Table 1, Entries 4, 8-9). To define the role and performance of $AlFeO_3@SiO_2@SO_3H$, the model reaction was carried out without the catalyst (Table 1, entry 10). The best results, in virtue of time and yield of reaction, was attained at 100 °C under solvent free medium and by using 10 mg of $AlFeO_3@SiO_2@SO_3H$ as a heterogeneous nanocatalyst (Table 1, entry 4).

With optimized condition in hand, the scope and limitation of this method was investigated for the desired products synthesis. As shown in scheme 2, the different aromatic aldehydes with electron-donating and electron-withdrawing substituents (**1a-f**) and dialdehydes (**1g-h**) were reacted with ethyl acetoacetate (**2**) and urea (**3**) to give the corresponding mono/bis 3,4-dihydropyrimidin-2-ones (**4a-h**) with good to excellent yields in short reaction times (Table 2). It was found that the reactions for all of the various substrates proceed efficiently to produce corresponding products in good yields without the formation of side products. All products were identified by comparison of their melting points and spectral data with those reported in the literature.

3.2.2. Selected spectroscopic data for dihydropyrimidin-2-one derivatives

Table 4.
Synthesis of 1,4-dihydropyridine derivatives in the presence of $AlFeO_3@SiO_2@SO_3H$ nanostructure.

Entry	Aldehydes	Product	Time (min.)	Yield[a] (%)	M.p[Ref]
1	4-Cl-C_6H_4CHO	**7a'**	15	95	221-225 [43]
2	4-OCH_3-C_6H_4CHO	**7b'**	45	92	236-238[43]
3	4-CH_3-C_6H_4CHO	**7c'**	40	93	254-256 [44]
4	4-OH-3-NO_2-C_6H_3CHO	**7d'**	60	90	-
5	4-CN-C_6H_4CHO	**7e'**	20	92	139-141[45]
6	terphethaldehyde	**7f'**	80	91	-
7	Isoterphetahldehyde	**7g'**	80	89	-
8	4,4'-(ethane-1,2-diylbis(oxy))dibenzaldehyde	**7h'**	120	80	-
9	4,4'-(propane-1,3-diylbis(oxy))dibenzaldehyde	**7i'**	120	85	-
10	2,2'-(propane-1,3-diylbis(oxy))dibenzaldehyde	**7j'**	120	85	-

[a] Isolated yield. Arylaldehyde (1mmol), ethyl acetoacetate (1mmol, 0.13 mL), dimedone (1 mmol, 0.14 g), ammonium acetate (1.5 mmol, 0.09 g), and the $AlFeO_3@SiO_2@SO_3H$ (10 mg) nanocatalyst under solvent free condition at 100 °C.

tives

Diethyl-4,4'-(1,4-phenylene)bis(6-methyl-2-oxo-1,2,3,4-tetrahydropyrimidine-5-carboxylate (**4g**): IR (KBr) (ν_{max}, cm^{-1}): 3324, 3240, 2975, 2933, 1703, 1646.; ^{1}H-NMR (300 MHz, DMSO-d_6) δ_H: 9.17 (s, 2H, NH), 7.16-7.69 (m, 6H, NH and H_{Ar}), 5.08 (s, 2H, CH), 3.96 (q, 4H, CH_2), 2.22 (S, 6H, CH_3), 1.08 (t, 6H, CH_3).; ^{13}C-NMR (75 MHz, DMSO-d_6) δ: 174.04, 165.77, 152.58, 148.74, 144.37, 126.76, 99.69, 59.67, 54.12, 18.23, 14.52.; Ms: (%): 442 (5), 260 (22), 231 (66), 183 (100), 155 (38).

Diethyl-4,4'-(1,3-phenylene)bis(6-methyl-2-oxo-1,2,3,4-tetrahydropyrimidine-5-carboxylate (**4h**): IR (KBr) (ν_{max}, cm^{-1}): 3283, 3216, 2959, 1703, 1611, 1491, 1379, 1218.; ^{1}H-NMR (300 MHz, DMSO-d_6) δ_H: 9.19 (s, 2H, NH), 7.22-7.74 (m, 6H, NH and H_{Ar}), 5.08 (s, 2H, CH), 3.97 (q, 4H, CH_2), 2.23 (s, 6H, CH_3) 1.08 (t, 6H, CH_3).; ^{13}C-NMR (75 MHz, DMSO-d_6) δ: 171.69, 165.79, 152.61, 148.82, 145.30, 128.85, 127.73, 126.70, 125.30, 99.71, 59.65, 54.41, 18.23, 14.52.; Ms: (%): 442 (8), 260 (90), 183 (100), 155 (33).

3.2.3. Catalytic activity of $AlFeO_3@SiO_2@SO_3H$ in the synthesis of 1,4-dihydropyridine derivatives (7a'-j')

The condition reaction was optimized as mentioned above (section 3.2.1). Different parameters of reaction including solvent, amount of nanocatalyst ($AlFeO_3@SiO_2@SO_3H$), and temperature were optimized in the model reaction of 4-chlorobenzaldehyde (1mmol, 0.14 g), ethyl acetoacetate (1mmol, 0.13 mL), dimedone (1 mmol, 0.14 g), and ammonium acetate (1.5 mmol, 0.09 g) (Table 3). The best results, in virtue of time and yield of reaction, was attained at 100 °C under solvent free medium and by using 10 mg of $AlFeO_3@SiO_2@SO_3H$ as a heterogeneous nanocatalyst (Table 3, entry 6). To define the role and performance of $AlFeO_3@SiO_2@SO_3H$, the model reaction was carried out without the catalyst and only 21% of desired product was achieved within 360 minutes (Table 1, entry 10).

After optimization of reaction condition, the scope and limitation of this procedure was considered for the desired products synthesis. As shown in scheme 2, the different aromatic aldehydes with electron-donating and electron-withdrawing substituents (**1a'-e'**) and dialdehydes (**1f'-j'**) were reacted with ethyl acetoacetate (**2**), dimedone (**5**), and ammonium acetate (**6**) to give the corresponding mono/bis 1,4-dihydropyridines (**7a'-j'**) with good to excellent yields (80-95%) in short reaction times (Table 4). It was found that the reactions for all of the various substrates proceed efficiently to produce corresponding products in good yields without the formation of side products. All products were identified by comparison of their melting points and spectral data with those reported in the literature.

3.2.4. Selected spectroscopic data for 1,4-dihydropyridine derivatives:

Diethyl-4,4'-(1,3-phenylene)bis(2,7,7-trimethyl-5-oxo-1,4,5,6,7,8-hexahydroquinoline-3-carboxylate) (**7g'**): IR (KBr) (ν_{max}, cm^{-1}): 3295, 3215, 3081, 2958, 1695, 1649, 1610, 1488, 1278, 1218.; ^{1}H-NMR (300 MHz, DMSO-d_6): δ_H = 0.98 (s, 12H, CH_3), 1.12 (t, 6H, J=3Hz, CH_3), 2.10-2.28 (m, 9H, CH_2, CH_3), 3.93 (s, 4H, CH_2), 4.79 (s, 2H, CH), 6.91 (d, 4H, J=33Hz, H_{Ar}), 8.99 (s, 2H, NH) ppm.; ^{13}C-NMR (75 MHz, DMSO-d_6) δ: 194.60, 167.27, 149.88, 147.80, 147.47, 145.82, 145.24, 126.89, 125.55, 125.11, 119.70, 110.47, 104.19, 103.48, 59.40, 50.76, 35.98, 35.32, 32.45, 29.63, 27.01, 18.77, 14.60 ppm.; Ms: (%): 600 (2), 561 (4), 188 (100), 160 (43).

Diethyl4,4'-((ethane-1,2-diylbis(oxy))bis(4,1-phenylene)) bis(2,7,7-trimethyl-5-oxo-1,4,5,6,7,8-hexahydroquinoline-3-carboxylate) (**7h'**): IR (KBr) (ν_{max}, cm^{-1}): 3275, 3078, 2959, 1703, 1645, 1606, 1491, 1277, 1218.; ^{1}H-NMR (300 MHz, DMSO-d_6): δ_H = 0.83 (s, 6H, CH_3), 0.99 (s, 6H, CH_3), 1.11 (t, 6H, J=3Hz, CH_3), 1.92-2.42 (m, 8H,

CH_2), 2.26 (s, 6H, CH_3), 3.95 (q, 4H, J=3Hz, CH_2), 4.16 (s, 4H, CH_2), 4.77 (s, 2H, CH), 6.75 (d, 4H, J=6Hz, H_{Ar}), 7.03 (d, 4H, J=3Hz, H_{Ar}), 9.01 (s, 2H, NH) ppm.; ^{13}C-NMR (75 MHz, DMSO-d_6) δ: 194.73, 167.36, 156.80, 154.16, 149.69, 145.19, 140.69, 138.15, 128.90, 114.09, 110.64, 107.81, 104.26, 35.39, 32.58, 29.61, 26.92, 18.72, 14.63 ppm.; Ms: (%): 736 (6), 475 (32), 262 (100), 234 (30), 205 (56).

Diethyl-4,4'-((propane-1,3-diylbis(oxy))bis(4,1-phenylene)) bis(2,7,7-trimethyl-5-oxo-1,4,5,6,7,8-hexahydroquinoline-3-carboxylate) (**7i'**): IR (KBr) ($\nu_{max,}$ cm^{-1}): 3289, 3080, 2958, 1698, 1608, 1490, 1381, 1218.; ^{1}H-NMR (300 MHz, DMSO-d_6): δ_H = 0.82 (s, 6H, CH_3), 0.98 (s, 6H, CH_3), 1.11 (t, 6H, CH_3), 1.92-2.42 (m, 13H, CH_2, CH_3), 3.91-4.01 (m, 8H, CH_2), 4.76 (s, 2H, CH), 6.73 (d, 4H, J=9Hz, H_{Ar}), 7.01 (d, 4H, J=9Hz, H $_{Ar}$), 9.00 (s, 2H, NH) ppm.; ^{13}C-NMR (75 MHz, DMSO-d_6) δ: 194.72, 167.37, 156.98, 149.66, 145.12, 140.53, 128.88, 114.07, 110.66, 104.32, 64.47, 59.44, 50.72, 35.38, 32.59, 29.60, 29.22, 26.95, 18.73, 14.63 ppm.; Ms: (%): 750 (4), 489 (24), 262 (100), 234 (28), 205 (24).

Diethyl4,4'-((propane-1,3-diylbis(oxy))bis(2,1-phenylene)) bis(2,7,7-trimethyl-5-oxo-1,4,5,6,7,8-hexahydroquinoline-3-carboxylate) (**7j'**): IR (KBr) ($\nu_{max,}$ cm^{-1}): 3275, 3203, 3078, 2959, 1695, 1607, 1280, 1217.; ^{1}H-NMR (300 MHz, DMSO-d_6): δ_H = 0.75 (d, 7H, CH_3), 0.95 (s, 6H, CH_3), 1.04 (t, 6H, J=3Hz, CH_3), 1.84-2.24 (m, 13H, CH_2, CH_3), 3.91-4.01 (m, 8H, CH_2), 5.06 (s, 2H, CH), 6.71-7.15 (m, 9H, H_{Ar}), 9.04 (d, 2H, J=9Hz, NH) ppm.; Ms: (%): 750 (5), 489 (22), 262 (100), 234 (47), 188 (31).

To prove the benefits of prepared hybrid magnetic nanocatalyst, we have compared its efficiency with other reported catalysts for synthesis of 3,4-dihydropyrimidin-2-one and 1,4-dihydropyridine derivatives in literature (Table 5). The presented data indicates the $AlFeO_3@SiO_2@SO3H$ is a suitable and an efficient comparable hybrid catalyst for the synthesis of desired 3,4-dihydropyrimidin-2-one and 1,4-dihydropyridine derivatives.

3.3. Recovery and reusability of $AlFeO_3@SiO_2@SO_3H$ in model reaction

The recovery and reusability of the catalysts are very important for commercial and industrial applications as well as green process aspects. Therefore, in this paper, the catalyst recyclability in model reaction for DHPs and DHPMs under the optimized reaction conditions were investigated. After completion of each reaction, the resulting solidified mixture was diluted with hot EtOH (15 mL). Then, the catalyst was easily separated, washed with hot EtOH, dried under vacuum, and reused in a subsequent reaction. Nearly, quantitative recovery of catalyst (up to 97%) could be obtained from each run. The recovered catalyst could be reused up to 5 cycles for synthesis of DHPs and DHPMs without any significant loss of activity (Figure 7). As seen, the FT-IR spectrum (Figure 7B), and XRD patterns (Figure 7C) of the catalyst after five runs confirmed its structure stability, integrity, and morphology.

Table 5.
Comparison of $AlFeO_3@SiO_2@SO_3H$ with other catalysts in the synthesis of 3,4-dihydropyrimidin-2-onea and 1,4-dihydropyridineb derivatives.

Table 5.

Entry	Product	Catalyst	Conditions	Time (min)	Yield[c] (%)	[Ref]
1	4a	[[Zn_2 (**5NO2-IP**)$_2$(**L**)$_2$] (H_2O)]$_n$ (ADES-**1**)	Solvent free, 80 ℃	10	94	[46]
2		WCHA-TG30	Solvent free, 130 ℃	14	94	[47]
3		Chloroferrate IL	Solvent free, 120 ℃	120	98	[48]
4		$AlFeO_3@SiO_2@SO_3H$	Solvent free, 100 ℃	45	97	This work
5	7a'	BNPs@$SiO_2(CH_2)_3$@NH-SO_3H	EtOH, Reflux	25	95	[49]
6		LAIL@MNP	Solvent-free Sonication, 80 ˚C	45	89	[50]
7		$AlFeO_3@SiO_2@SO_3H$	Solvent free, 100 ˚C	30	95	This work

[a] Benzaldehyde, ethyl acetoacetate, urea, and $AlFeO_3@SiO_2@SO_3H$ nanocatalyst
[b] 4-Chlorobenzaldehyde, ethyl acetoacetate, dimedone, ammonium acetate, and the $AlFeO_3@SiO_2@SO_3H$ nanocatalyst.
[c] Isolated yield.

4. Conclusions

An innovative and effective sulfonic acid-decorated aluminium ferrite ($AlFeO_3@SiO_2@SO_3H$) nanostructure was fabricated and characterized. The prepared perovskite-based hybrid nanostructure indicated good catalytic activity in the synthesis of several mono/bis dihydropyrimidin-2-one and 1,4-dihydropyridine derivatives using Biginelli and Hantzsch MCRs. Besides, the $AlFeO_3@SiO_2@SO_3H$ could be reused for five runs without a significant decrease in its catalytic activity. High isolated yield of pure products, good thermal and chemical stability of hybrid nanocatalyst, easy work-up procedure, reusability of the catalyst and green reaction condition are the remarkable advantages of this protocol. The results revealed the performance of $AlFeO_3@SiO_2@SO_3H$ is comparable to many reported catalysts in terms of yield, reaction time and green condition.

Acknowledgement

We gratefully want to acknowledge the partial financial support of this work from the research council of Arak University.

REFERENCES

[1] P. Costanzo, M. Nardi, M. Oliverio, Similarity and competition between Biginelli and Hantzsch reactions: an opportunity for modern medicinal chemistry, European Journal of Organic Chemistry 2020(26) (2020) 3954-3964.
[2] S.M. Gomha, Z.A. Muhammad, H.M. Abdel-aziz, I.K. Matar, A.A. El-Sayed, Green synthesis, molecular docking and anticancer activity of novel 1, 4-dihydropyridine-3, 5-Dicarbohydrazones under grind-stone chemistry, Green Chemistry Letters and Reviews 13(1) (2020) 6-17.
[3] S. Faizan, B.P. Kumar, N.L. Naishima, T. Ashok, A. Justin, M.V. Kumar, R.B. Chandrashekarappa, N.M. Raghavendra, P. Kabadi, L. Adhikary, Design, parallel synthesis of Biginelli 1, 4-dihydropyrimidines using PTSA as a catalyst, evaluation of anticancer activity and structure activity relationships via 3D QSAR studies, Bioorganic Chemistry 117 (2021) 105462.
[4] P. Michalska, P. Mayo, C. Fernández-Mendívil, G. Tenti, P. Duarte, I. Buendia, M.T. Ramos, M.G. López, J.C. Menéndez, R. León, Antioxidant, anti-inflammatory and neuroprotective profiles of novel 1, 4-dihydropyridine derivatives for the treatment of Alzheimer's disease, Antioxidants 9(8) (2020) 650.
[5] N. Khaldi-Khellafi, M. Makhloufi-Chebli, D. Oukacha-Hikem, S.T. Bouaziz, K.O. Lamara, T. Idir, A. Benazzouz-Touami, F. Dumas, Green synthesis, antioxidant and antibacterial activities of 4-aryl-3, 4-dihydropyrimidinones/thiones derivatives of curcumin. Theoretical calculations and mechanism study, Journal of Molecular Structure 1181 (2019) 261-269.
[6] A. Malani, A. Makwana, J. Monapara, I. Ahmad, H. Patel, N. Desai, Synthesis, molecular docking, DFT study, and in vitro antimicrobial activity of some 4-(biphenyl-4-yl)-1, 4-dihydropyridine and 4-(biphenyl-4-yl) pyridine derivatives, Journal of Biochemical and Molecular Toxicology 35(11) (2021) e22903.
[7] V. Ramachandran, K. Arumugasamy, S.K. Singh, N. Edayadulla, P. Ramesh, S.-K. Kamaraj, Synthesis, antibacterial studies, and molecular modeling studies of 3, 4-dihydropyrimidinone compounds, Journal of chemical biology 9(1) (2016) 31-40.
[8] B. Borah, M. Patat, S. Swain, L.R. Chowhan, Recent advances and prospects in the transition-metal-free synthesis of 1, 4-dihydropyridines, ChemistrySelect 7(27) (2022) e202202484.

[9] L.H.S. Matos, F.T. Masson, L.A. Simeoni, M. Homem-de-Mello, Biological activity of dihydropyrimidinone (DHPM) derivatives: A systematic review, European journal of medicinal chemistry 143 (2018) 1779-1789.
[10] R. Janis, P. Silver, D. Triggle, Drug action and cellular calcium regulation, Advances in drug research 16 (1987) 309-591.
[11] E. Khanina, G. Silinietse, Y. Ozol, G.Y. Dubur, A. Kimenis, Synthesis and pharmacological investigation of some derivatives of 1, 2, 3, 4-tetrahydropyrimidine-5-carboxylic acid, Pharmaceutical Chemistry Journal 12(10) (1978) 1321-1323.
[12] B.H. Rotstein, S. Zaretsky, V. Rai, A.K. Yudin, Small heterocycles in multicomponent reactions, Chemical reviews 114(16) (2014) 8323-8359.
[13] B. Borah, J. Bora, P. Ramesh, L.R. Chowhan, Sonochemistry in an organocatalytic domino reaction: an expedient multicomponent access to structurally functionalized dihydropyrano [3, 2-b] pyrans, spiro-pyrano [3, 2-b] pyrans, and spiro-indenoquinoxaline-pyranopyrans under ambient conditions, RSC advances 12(20) (2022) 12843-12857.
[14] A. Hantzsch, Ueber die synthese pyridinartiger verbindungen aus acetessigäther und aldehydammoniak, Justus Liebigs Annalen der Chemie 215(1) (1882) 1-82.
[15] Z. Hajizadeh, A. Maleki, J. Rahimi, R. Eivazzadeh-Keihan, Halloysite nanotubes modified by Fe3O4 nanoparticles and applied as a natural and efficient nanocatalyst for the symmetricalhantzsch reaction, Silicon 12(5) (2020) 1247-1256.
[16] M. Najjar, M.A. Nasseri, M. Darroudi, A. Allahresani, Synthesis of dihydropyrimidinone and dihydropyridine derivatives by a GQDs-based magnetically nanocatalyst under solvent-free conditions, Journal of Environmental Chemical Engineering 10(6) (2022) 108854.
[17] M.A. Ashraf, Z. Liu, W.-X. Peng, C. Gao, New copper complex on Fe_3O_4 nanoparticles as a highly efficient reusable nanocatalyst for synthesis of polyhydroquinolines in water, Catalysis Letters 150(3) (2020) 683-701.
[18] P. Kamalzare, B. Mirza, S. Soleimani-Amiri, Chitosan magnetic nanocomposite: a magnetically reusable nanocatalyst for green synthesis of Hantzsch 1, 4-dihydropyridines under solvent-free conditions, Journal of Nanostructure in Chemistry 11(2) (2021) 229-243.
[19] S. Rezayati, F. Kalantari, A. Ramazani, S. Sajjadifar, H. Aghahosseini, A. Rezaei, Magnetic Silica-Coated Picolylamine Copper Complex [Fe_3O_4@ SiO_2@ GP/Picolylamine-Cu (II)]-Catalyzed Biginelli Annulation Reaction, Inorganic chemistry 61(2) (2021) 992-1010.
[20] S.F. Taheri Hatkehlouei, B. Mirza, S. Soleimani-Amiri, Solvent-free one-pot synthesis of diverse dihydropyrimidinones/tetrahydropyrimidinones using biginelli reaction catalyzed by Fe_3O_4@ C@ OSO_3H, Polycyclic Aromatic Compounds (2020) 1-17.
[21] A. Allahresani, M. Mohammadpour Sangani, M.A. Nasseri, $CoFe_2O_4$@ SiO2-NH_2-CoII NPs catalyzed Hantzsch reaction as an efficient, reusable catalyst for the facile, green, one-pot synthesis of novel functionalized 1, 4-dihydropyridine derivatives, Applied Organometallic Chemistry 34(9) (2020) e5759.
[22] N. Devarajan, P. Suresh, MIL-101-SO_3 H metal–organic framework as a Brønsted acid catalyst in Hantzsch reaction: an efficient and sustainable methodology for one-pot synthesis of 1, 4-dihydropyridine, New Journal of Chemistry 43(17) (2019) 6806-6814.
[23] H. Alinezhad, K. Pakzad, Green synthesis of copper oxide nanoparticles with an extract of Euphorbia Maculata and their use in the Biginelli reaction, Organic Preparations and Procedures International 52(4) (2020) 319-327.
[24] B.-J. Yao, W.-X. Wu, L.-G. Ding, Y.-B. Dong, Sulfonic Acid and Ionic Liquid Functionalized Covalent Organic Framework for Efficient Catalysis of the Biginelli Reaction, The Journal of Organic Chemistry 86(3) (2021) 3024-3032.
[25] L.H. da Silveira Lacerda, R.A.P. Ribeiro, S.R. de Lazaro, Magnetic, electronic, ferroelectric, structural and topological analysis of $AlFeO_3$, $FeAlO_3$, $FeVO_3$, $BiFeO_3$ and $PbFeO_3$ materials: theoretical evidences of magnetoelectric coupling, Journal of Magnetism and Magnetic Materials 480 (2019) 199-208.
[26] S. Bhuvanasundari, G. Venkatachalam, M. Doble, T. Thomas, Magnetically recoverable, non-toxic, leach resistant aluminum ferrite ($AlFeO_3$) photocatalyst for wastewater remediation, Ceramics International 48(21) (2022) 32326-32337.
[27] F.Z. Kassimi, H. Zaari, A. Benyoussef, A. Rachadi, M. Balli, A. El Kenz, A theoretical study of the electronic, magnetic and magnetocaloric properties of the $TbMnO_3$ multiferroic, Journal of Magnetism and Magnetic Materials 543 (2022) 168397.
[28] N.A. Hill, Why are there so few magnetic ferroelectrics?, ACS Publications, 2000, pp. 6694-6709.
[29] R. Saha, A. Sundaresan, C. Rao, Novel features of multiferroic and magnetoelectric ferrites and chromites exhibiting magnetically driven ferroelectricity, Materials Horizons 1(1) (2014) 20-31.
[30] Q. Li, S. Wang, Y. Yuan, H. Gao, X. Xiang, Phase-controlled synthesis, surface morphology, and photocatalytic activity of the perovskite $AlFeO_3$, Journal of Sol-Gel Science and Technology 82 (2017) 500-508.
[31] N. Ahadi, A. Mobinikhaledi, M.A. Bodaghifard, One-pot synthesis of 1, 4-dihydropyridines and N-arylquinolines in the presence of copper complex stabilized on $MnFe_2O_4$ (MFO) as a novel organic–inorganic hybrid material and magnetically retrievable catalyst, Applied Organometallic Chemistry 34(10) (2020) e5822.
[32] H. Moghanian, M.A.B. Fard, A. Mobinikhaledi, N. Ahadi, Bis (p-sulfoanilino) triazine-functionalized silica-coated magnetite nanoparticles as an efficient and magnetically reusable nano-catalyst for Biginelli-type reaction, Research on Chemical Intermediates 44(7) (2018) 4083-4101.
[33] N. Foroughifar, A. Mobinikhaledi, S. Ebrahimi, H. Moghanian, M.A.B. Fard, M. Kalhor, Synthesis of a new class of azathia crown macrocycles containing two 1, 2, 4-triazole or two 1, 3, 4-thiadiazole rings as subunits, Tetrahedron Letters 50(7) (2009) 836-839.
[34] L.B. Farhat, S.B. Ahmed, S. Ezzine, M. Amami, Particle size dependent structural, magnetic and electrical properties of Cr-doped lead-free multiferroic $AlFeO_3$ prepared by co-precipitation and solid state method, Materials Chemistry and Physics 255 (2020) 123631.
[35] J. Safaei-Ghomi, H. Shahbazi-Alavi, A flexible one-pot synthesis of pyrazolopyridines catalyzed by Fe3O4@ SiO_2-SO_3H nanocatalyst under microwave irradiation, Scientia Iranica 24(3) (2017) 1209-1219.
[36] C.S. Maldonado, D. la Rosa, J. Rivera, C.J. Lucio-Ortiz, A. Hernández-Ramírez, F.F.C. Barraza, J.S. Valente, Low concentration Fe-doped alumina catalysts using sol-gel and impregnation methods: the synthesis, characterization and catalytic performance during the combustion of trichloroethylene, Materials 7(3) (2014) 2062-2086.
[37] R. Saha, A. Shireen, S.N. Shirodkar, M.S. Singh, U.V. Waghmare, A. Sundaresan, C. Rao, Phase Transitions of $AlFeO_3$ and $GaFeO_3$ from the Chiral Orthorhombic (Pna 21) Structure to the Rhombohedral ($R^{\bar{3}}c$) Structure, Inorganic chemistry 50(19) (2011) 9527-9532.
[38] Q. Li, S. Wang, Y. Yuan, H. Gao, X. Xiang, Phase-controlled synthesis, surface morphology, and photocatalytic activity of the perovskite $AlFeO_3$, Journal of Sol-Gel Science and Technology 82(2) (2017) 500-508.